Front. Electr. Electron. Eng. China (2006) 3: 350–354
DOI 10.1007/s11460-006-0028-x

RESEARCH ARTICLE

XU Yue-tong, FU Jian-zhong, CHEN Zi-chen

Thrust ripple optimization and experiment for a permanent magnet linear synchronous motor

Abstract Thrust ripple such as end force, slot force and normal force are key factors that affect the properties of permanent magnet linear synchronous motors (PMLSM). According to different mechanics and analytical models, end force resulting from open magnetic circuit of PMLSM was greatly decreased by optimizing the length of the PMLSM mover. Slot force caused by slot effect was greatly reduced by using fraction slot structure, and normal force was calculated through the finite element method (FEM). After thrust ripple was calculated, its uniform formula was obtained through Fourier series nonlinear regression. An experimental system was set up to measure thrust ripple, and experiment results demonstrated that experimental force ripple was quite in line with that calculated by the fitting formula. The optimal theory and analysis method is effective, and the obtained formula can be utilized to compensate thrust ripple in practical applications and improve the motion performance of PMLSM.

Keywords PMLSM, end force, slot force, normal force

1 Introduction

High-speed machining and micro-fabrication represent important development trends in mechanical manufacture and science research [1–3], which require high-performance feeding systems with high-performance, such as major thrust, high-frequency response, and good motion properties etc.. The main benefits arising from the use of PMLSM include the high thrust density, low thermal losses, short electrical time-constant, rapid velocity response and, most importantly, the high precision and accuracy achievable from the simplicity in mechanical structure [4]. PMLSM drives are superior to other drives, such as gearboxes, chains, and screws coupling, because of their high-speed, precision positioning, and compact structure. This makes PMLSM more and more applicable in machine tools, micro-fluidic chip manufacturing, semiconductor wafer manufacturing and so on [5–7].

Unfortunately, PMLSM have a few disadvantages which have some adverse effects on its performance, such as:

1) There will be a large end force in PMLSM because of open magnetic field if it isn't designed properly.

2) Numerous q, the number of slots per phase on one pole pitch, is not possible for PMLSM because of its short pole pitch, and it also can not be designed as an small integer. If it was, the harmonic component of magnetic fields through winding layout could not be reduced and PMLSM might have a rather large slot force.

3) Compared with its thrust, PMLSM has a rather large normal force to induce additional friction force. These forces make thrust ripple produce both vibration and noise, and deteriorate the control characteristics of speed control at low speed as well as of position control. Particularly at the moment of brake, thrust ripple will make PMLSM drives deviate from their target location, reduce machining precision, and may even induce oscillating and consequently decrease the lifetime of electronic devices. Many studies have been performed to decrease the adverse effects of thrust ripple. For example, the Halbach array of permanent magnet was developed to realize an ideal magnetic field, but increased manufacturing difficulty [8]; a basic analytic model but not an exact model of force ripple was built and an opposing waveform of the force ripple was developed at the other end based on the assumption that force ripple is symmetrical about its peak [9]; Jeans et al. [10] adopted the analytic model in the statement [10] and optimized the length of the mover to reduce the ripple directly by utilizing phase difference method; and Li and Wang [11] analyzed force ripple arising from end effect but didn't build any

Translated from *Proceeding of the Chinese Society for Electrical Engineering*, 2005, 25(12): 122–126 (in Chinese)

XU Yue-tong (✉), FU Jian-zhong, CHEN Zi-chen
The Institute of Advanced Manufacturing Engineering,
Zhejiang University, Hangzhou 310027, China
E-mail: xyt@zju.edu.cn

analytic model and present any simulation results.

This paper presents optimal design methods to reduce force ripples. First, the model of end force was built, and the length of the mover was optimized to reduce end force after it was calculated through Fourier series nonlinear regression and numeric method. Then fraction slot structure was designed for PMLSM to decrease higher harmonic wave and reduce slot force in it. Normal force was calculated through FEM. And consequently the uniform formula of force ripple was obtained through Fourier series nonlinear regression. Finally the measurement of the force ripple was conducted within one pole pitch to confirm the effectiveness of the technique.

2 Optimal design for thrust ripple of PMLSM

2.1 Optimal design for end force of PMLSM

Table 1 shows the main parameters of the designed PMLSM whose mover length is originally set as 23τ and finally determined by the result of optimal design.

Table 1 Brief specification of PMLSM

	Item	Symbol	Value (Unit)
	No. of phase	m	3
	Slot width	w_s	6.67/mm
Primary	Slot pitch	τ_s	14.57/mm
core	Slot height		29.5/mm
	No. of slot		24
	Pole pitch	τ	16/mm
Permanent	Length x width x height		50×14×24 / mm
magnet	Residual	B_r	1.2 / T
Air gap	Mechanical air gap	g_m	0.8/mm

End force results from the finite length of the mover. When the mover is longer than 2–3 pole pitches, the left-hand end force f_l is not influenced by the the right-hand f_r approximately, so the resultant end force is simply the sum of f_l and f_r. With same amplitude and characteristic but opposite direction due to non-uniform magnetic field at each end, f_l and f_r are functions of position and periodic over every slot pitch. There is a phase difference that is determined by the length of the mover between f_l and f_r, but their phase difference is not the same as that of geometric structure [12]

$$f_l(x) = -f_r(-x-\lambda) \tag{1}$$

where $\lambda = k\tau - L_s$, L_s being the mover length, k any integer. f_l and f_r can be expressed in the form of a Fourier series

$$\begin{cases} f_l(x) = f_0 + \sum_{n=1}^{\infty}(f_{sn}\sin\frac{2n\pi}{\tau}x + f_{cn}\cos\frac{2n\pi}{\tau}x) \\ f_r(x) = -f_0 + \sum_{n=1}^{\infty}(f_{sn}\sin\frac{2n\pi}{\tau}(x+\lambda) - f_{cn}\cos\frac{2n\pi}{\tau}(x+\lambda)) \end{cases} \tag{2}$$

Therefore the resultant end force of PMLSM whose mover length $L_s = k\tau - \lambda$ is obtained as

$$f_{end}(x) = f_l + f_r = \sum_{n=1}^{\infty} f_{en}\sin\frac{2n\pi}{\tau}(x+\frac{\lambda}{2}) \tag{3}$$

where $f_{en} = (f_{sn}\cos\frac{n\pi\lambda}{\tau} + f_{cn}\sin\frac{n\pi\lambda}{\tau})$.

From Eq. (3), we can see that the resultant end force is the function of λ, and the optimal λ_{opt} to minimize the fundamental wave of the resultant end force can be obtained from Eq. (3) as

$$\lambda_{opt} = \frac{\tau}{\pi}\arctan(-\frac{f_{sn_1}}{f_{cn_1}}) \tag{4}$$

The left-hand end force can be calculated on the displacement of one pole pitch by Maxwell's tensor analysis after the magnetic field is computed by finite-element method. Its waveform can be curve fitted by Fourier series nonlinear regression as:

$$\begin{aligned} f_l = {} & 25.701\,7 + 16.370\,2\sin(\frac{2\pi}{16}x) + 4.570\,1\sin(\frac{4\pi}{16}x) \\ & + 1.434\,2\sin(\frac{6\pi}{16}x) + 0.426\,2\sin(\frac{8\pi}{16}x) \\ & - 3.512\,5\cos(\frac{2\pi}{16}x) - 0.317\,1\cos(\frac{4\pi}{16}x) \\ & - 0.118\,0\cos(\frac{6\pi}{16}x) - 0.124\,4\cos(\frac{8\pi}{16}x) + \cdots \end{aligned} \tag{5}$$

From Eqs. (2), (4), and (5), the optimal λ_{opt} and the resultant end force of the original PMLSM can be obtained respectively as:

$$\lambda_{opt} = \frac{16}{\pi}\arctan(\frac{16.370\,2}{3.515\,2}) = 7.912 \tag{6}$$

$$\begin{aligned} f_{end} = {} & 2\,[16.370\,2\sin(\frac{2\pi}{16}x) + 4.570\,1\sin(\frac{4\pi}{16}x) \\ & + 1.434\,2\sin(\frac{6\pi}{16}x) + 0.426\,2\sin(\frac{8\pi}{16}x) + \cdots] \end{aligned} \tag{7}$$

Considering the symmetry of the PMLSM winding λ_{opt} is set as 8 mm, the half of pole pitch, and consequently the optimal mover length $L_s = 23\,\tau - \lambda_{opt} = 360$ mm. As can be seen from Eq. (2), the resultant end force after optimization doesn't contain odd items of sine wave and even items of cosine wave, and its coefficients is determined by Eq. (5), so it can be expressed as:

$$\begin{aligned} f_{opt}(x) = {} & 2\,[4.570\,1\sin(\frac{4\pi}{16}x) + 0.426\,2\sin(\frac{8\pi}{16}x) \\ & + \cdots - 3.512\,5\cos(\frac{2\pi}{16}x) - 0.118\,0\cos(\frac{6\pi}{16}x) + \cdots] \end{aligned} \tag{8}$$

Figure 1 compares the calculated end force on one pole pitch corresponding to both the original mover length L_s and the optimal mover length L_{opt}. From Fig. 1, the maximum end force of 35 N is reduced to 15 N approximately by optimizing the mover length.

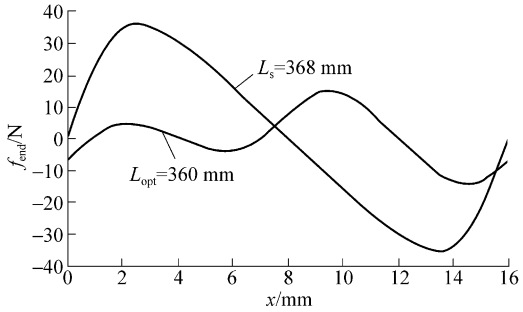

Fig. 1 The end force contrast sketch between the optimized length and the primary length

2.2 Optimal design for slot force of PMLSM

PMLSM has many poles and consequently pole pitch is small, so numerous q (the number of slots per phase on one pole pitch) can not usually be applied for easy manufacturing purpose, and q can not be designed as a small integer. If it was, harmonic component of magnetic fields could not be reduced through winding layout. Furthermore, lower harmonic components with high amplitudes are significant when q is set as a small integer. So q is designed as a fractional number but not an integer in our case. The designed PMLSM has 24 slots, 14.67 mm slot pitch and 16 mm pole pitch. The number of poles and the angle of slot pitch can be calculated respectively as

$$\begin{cases} p = \dfrac{14.67 \times 24}{16} = 22 \\ \alpha = \dfrac{14.67 \times 180°}{16} = 165° \end{cases} \tag{9}$$

From Eq. (9), the designed PMLSM is equivalent to a double-pole motor with 4 slots per phase on one pole pitch and an electrical angle $\alpha' = 15^{\circ}$. With single-layer winding whose coefficient $k_p = 1$, the winding coefficient of the designed PMLSM can be computed by

$$k_w = k_p k_b = \frac{\sin\dfrac{q'\alpha'}{2}}{q'\sin\dfrac{\alpha'}{2}} = \frac{\sin 30^{\circ}}{4\sin 7.5^{\circ}} = \frac{0.5}{4 \times 0.130\,5} = 0.957\,7 \tag{10}$$

From Eq. (10), applying fractional slot winding can abate higher harmonic components and therefore reduce the slot force. To check the influence of fractional slot winding to slot force, we can use periodic continuation of slots of the mover to eliminate the influence of end effect and calculate the slot force on the displacement of one pole pitch by method of virtual work after the magnetic field was computed by finite-element method. Figures 2 and 3 show the calculated slot force of fractional slot structure and one slot on one pitch structure respectively.

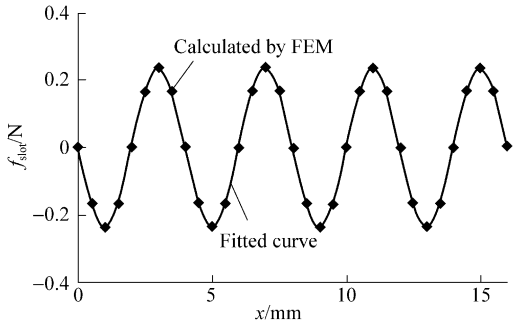

Fig. 2 Slot force of PMLSM with fraction structure

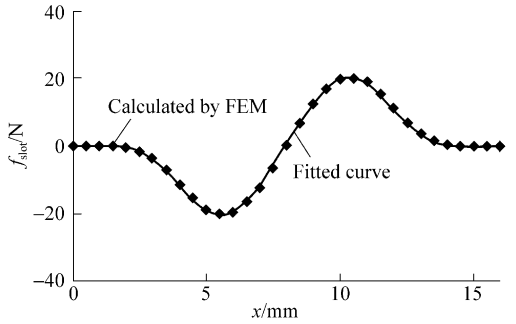

Fig. 3 Slot force of PMLSM when slot pitch is equal to pole pitch

From Figs. 2 and 3, the maximum slot force of 20.5 N is reduced to 0.22 N approximately by applying fractional slot. Its waveform can be curve fitted by Fourier series nonlinear regression as

$$f_{\text{slot}}(x) = -0.232\sin\left(\frac{8\pi x}{16}\right) \tag{11}$$

3 Calculation of friction force by finite-element method

The friction force in PMLSM results from both the mover inertia and normal force. Since normal force is much larger than magnetic thrust [13], it must be carefully analyzed. On the basis of the optimal mover length and fractional slot structure, after the magnet vector potential is computed by

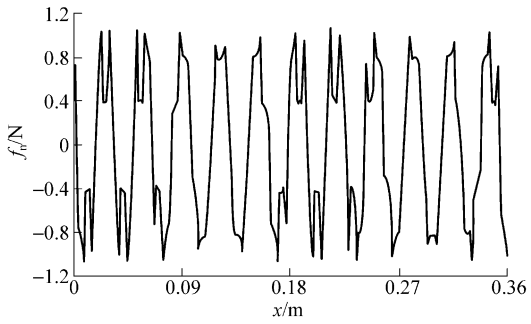

Fig. 4 Magnet flux contribution on the armature surface of PMLSM caused by permanent magnet

finite-element method, the distribution of magnetic flux intensity in PMLSM can be calculated by post processor, as show in Fig. 4. Then normal force can be calculated on the displacement of one pole pitch by method of virtual work, as show in Fig. 5.

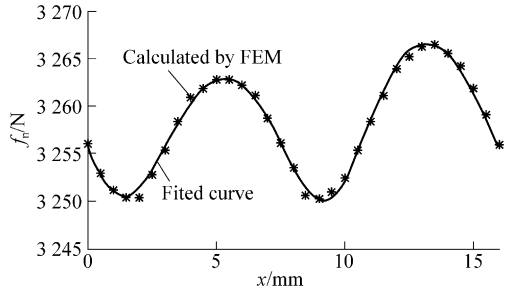

Fig. 5 Normal force distribution on one pole pitch

From Fig. 2, no-load normal force waveform can be curve fitted by Fourier series nonlinear regression as:

$$\begin{aligned} f_n = {} & 325.2 - 1.16\sin(\frac{\pi}{8}x) - 6.16\sin(\frac{\pi}{4}x) \\ & - 0.05\sin(\frac{3\pi}{8}x) - 0.52\sin(\frac{\pi}{2}x) + 0.95\cos(\frac{\pi}{8}x) \\ & - 3.74\cos(\frac{\pi}{4}x) + 0.34\sin(\frac{3\pi}{8}x) + 0.30\cos(\frac{\pi}{2}x) + \cdots \end{aligned} \tag{12}$$

Considering the friction coefficient of linear guide rail in our PMLSM $\mu_m = 0.01$ and the mover inertial $m = 30$ kg, the total sliding-friction force can be expressed as

$$\begin{aligned} f_m &= \mu_m(f_n + mg) \\ &\approx 35.52 - 0.06\sin(\frac{\pi}{4}x) - 0.04\cos(\frac{\pi}{4}x) \end{aligned} \tag{13}$$

From Eqs. (8), (11) and (13), the total thrust ripple can be obtained as

$$\begin{aligned} f(x) = {} & 35.52 + 9.18\sin(\frac{\pi}{4}x) + 0.62\sin(\frac{\pi}{2}x) \\ & - 0.04\cos(\frac{\pi}{4}x) - 7.02\cos(\frac{\pi}{8}x) - 0.236\cos(\frac{3\pi}{8}x) \end{aligned} \tag{14}$$

4 Experiment for thrust ripple in PMLSM

Figure 6 shows the overall experimental system set up for measurement of thrust ripple in PMLSM. The system consists of a control box, a PMLSM drive, and several measuring apparatus. The control box consists of a transformer, a 24 V DC power supplier, a motor driver, several contactors, a power-wasting resistance, and a computer etc., The PMLSM drive includes a PMLSM, an encoder with resolution 1 μm, a pair of limit switches, a zero switch, and a pair of linear guide rail and so on. The PMLSM used in this experiment has the following parameters: electrical resistance R = 5.3 Ω(L–L), electrical inductance L = 53.4 mH (L–L), permanent magnet (PM) material: NdFeB, the pole pitch of PM τ = 16 mm, the gap between the mover and PM δ = 0.8 mm and the maximum traveling distance: 240 mm.

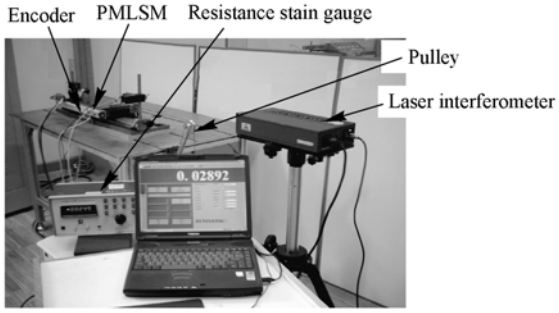

Fig. 6 Thrust ripple measurement system of PMLSM

A laser interferometer, a resistance stain gauge, a rope, a pulley and an adjustable load are set up to measure thrust ripple. When load is added gradually until the reading of the laser interferometer begins to change, the reading of the resistance stain gauge is namely the thrust ripple of PMLSM at this point. Figure 7 shows the thrust ripple of PMLSM on one pole pitch.

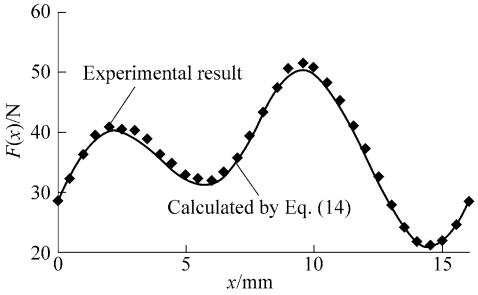

Fig. 7 Thrust ripple distribution on one pole pitch of PMLSM

Figure 7 demonstrates that experimental force ripple was quite in line with that calculated by the fitting Eq. (14). So the optimal theory and analysis method is effective.

5 Conclusions

Thrust ripple in PMLSM has been greatly reduced by optimizing the mover length and applying fractional slot structure after analyzing their mechanics. Fitting curve of thrust ripple had been obtained after end force, slot force and friction force are calculated. Experiment result demonstrated that the measured force ripple was in line with that calculated by the fitting formula approximately, verifying that the optimal theory and analysis method are effective. Hence the fitting curve can be utilized to compensate thrust ripple in practice in order to improve servo performance of the PMLSM drive, such as improving its positioning accuracy and enhancing the steadiness of its velocity response etc..

Acknowledgements This study was supported by the National Natural Science Foundation of China (No. 50475101).

References

1. Guo K. H., Ren L. et al., Standardization of field emission measurement, J. Vac. Sci. Technol., 2001, B19(1): 87–93
2. Liu Jian-fang, Yang Zhi-gang, Cheng Guang-ming et al., A study of precision pzt line step motor, Proceeding of the CSEE, 2004, 24(4): 102–107
3. Ji Ke-hui, Guo Ji-fang, Liu Xiao, Stepping characteristic of ultrasonic motor and its stepping-positioning control, Proceeding of the CSEE, 2004, 24(1): 71–75
4. Xia Jia-kuan, Wang Cheng-yuan, Li Hao-dong et al., Study of end-effects analysis and NN compensation technique of linear motor for high precision NC machine, Proceeding of the CSEE, 2003, 23(8): 100–104
5. Ye Yun-yue, The Theory and Application of Linear Motors, Beijing: Mechanical Industry Press, 2000, 127–129
6. Jiao Liu-cheng, Yuan Shi-ying, Evaluation of equivalent parameters for permanent magnet linear synchronous motor for vertical movement, Proceeding of the CSEE, 2002, 22(3): 12–16
7. Jiao Liu-cheng, Yuan Shi-ying, Study on the operating characteristic permanent magnet linear synchronous motor for vertical movement, Proceeding of the CSEE, 2002, 22(4): 37–40
8. Xu Yue-tong, Fu Jian-zhong, Chen Zi-chen, Precise and robust control of permanent magnet linear synchronous motors in a high-speed feeding system, Proceedings of Fifth World Congress on Intelligent Control and Automation, 2004, Hangzhou, China, 6(5): 4516–4520
9. Lee Sung Ho, Yoon In Ki, Design criteria for detent force reduction of permanent-magnet linear synchronous motors with Halbach array, International Magnetics Conference, 2002, Amsterdam, Netherlands, 38: 3261–3263
10. Zhu, Z. O, Xia Z. P, Howe D., Mellor, P. H., Reduction of cogging force in slotless linear permanent magnet motors, Electric Power Applications, IEE Proceedings, 1997, 144(4): 277–282
11. Jeans C. G, Cruise R. J, Landy C. F., Methods of detent force reduction in linear synchronous motors, International Conference IEMD '99, 1999, Seattle, WA USA
12. Li Qing-lei, Wang Xian-kui, Thrust fluctuation analysis and reduction of PMLSM, Tsinghua Univ(Sci and Tech), 2000, 40(5): 33–36
13. Pan Kai-lin, Fu Jian-zhong, Chen Zi-chen, Detent force analysis and reduction of PMLSM, Proceeding of the CSEE, 2004, 24(4): 112–115
14. Boldea I, Nasar S. N., Linear electric actuators and generators, Cambridge: Cambridge University Press, 1997, 111–115